Research Article – Vol. 01, Issue 01, No. 05

Advanced in Engineering and Intelligence Systems

Journal Web Page: https://aeis.bilijipub.com

Determining the amount of earthquake displacement using differential synthetic aperture radar interferometry (D-InSAR) and satellite images of Sentinel-1 A: A case study of Sarpol-e Zahab city

Jacob Cherian[1,*]

[1] *College of Business, Abu Dhabi University, Abu Dhabi P.O. Box 59911, United Arab Emirates*

Highlights

- Radar data of SAR from the Sentinel-1 A satellite were prepared before and after the earthquake for the case study area.
- The removal of existing noises was done by the interferogram generated from the Goldstein filter, and absolute generated phase were changed to displacement.
- After processing the data, the processed data were georeferenced to study the relevant images in the coordinates of the analyzed area.
- The results of this study showed that maximum displacement occurred in the north and northwest of the city
- It's suggested to use radar data such as Sentinel-1 to investigate displacement of the land surface.

Article Info

Received: 17 January 2022
Received in revised: 04 april 2022
Accepted: 04 april 2022
Available online: 16 April 2022

Keywords

Land displacement
Earthquake
Sentinel-1 A satellite
D-INSAR method
Sarpol-e Zahab city

Abstract

One of the effects of an earthquake is the creation of displacement on the land surface. It's important to determine displacement due to natural disasters such as earthquakes. So, it's essential to identify height changes occurring on Earth due to these movements. Detecting these changes in the extent of field operations requires a lot of time and money; hence, satellite technology can be used to eliminate the limitations of field operations. This study aimed to determine the trend and rate of land surface changes in the Sarpol-e Zahab earthquake using Sentinel-1 A and D-InSAR method. To this end, two radar images of SAR from the Sentinel-1 A satellite were prepared before and during the earthquake. Then, these two images were registered based on a prepared radar file to produce the interferogram of study area. After removing the topography phase, the removal of existing noises was done by the interferogram generated from the Goldstein filter. Then, to determine the real phase difference, the produced phases were corrected. Before changing phase to displacement, to improve the processing results, the refining phase and applying multiple corrections and absolute generated phase were changed to displacement. The displacement map of Sarpol-e Zahab city resulted from an earthquake of 7.3 magnitudes showing displacement between -1.6 and 68 centimeters. Also, the results of this study showed that maximum displacement occurred in the north and northwest of the city, namely the villages of Dasht-e Zahab, Sarpol suburb, and Posht-tang, because of the adjacency of the earthquake center. Given the advantages of using remote sensing data, such as the ability to check the displacement between any desired point with the proper precision on the interferogram and the extensive coverage of SAR images, it's suggested to use radar data such as Sentinel-1 to investigate displacement of the land surface.

1. Introduction

Earthquake is a natural and hazardous phenomenon for most of the world's inhabitants, which has caused the greatest damage to humanity so far [1]. As it is situated on the earthquake belt, Iran is considered a risky zone where a destructive earthquake occurs in each decade. The earthquakes in Boeing Zahra, Ferdows and Qaenat in the 40th, Tabas, Qaenat, and Khaf in the 50th, Manjil and Bojnourd in the 60th, Ardebil, Qaenat and Changure in the 70th, Bam, Firoozabad, and Zaradn in the early 80th, and finally Kermanshah earthquake are some examples of the important earthquakes in this country. Earthquake is due to tectonic activity at the boundary between the Earth's crust plates. These tectonic behaviors lead to different

* Corresponding Author: Jacob Cherian
Email: jacob.cherian@adu.ac.ae

spatial and temporal behaviors in the Earth's crust, one of the most important of which is the creation of displacement on the Earth's surface. This displacement can cause damage to the structure of buildings, runways [2], bridges, tunnels, streets, railways and roads [3], agricultural facilities, disturbances in the flow pattern of hydrology [4], the degradation of electrical ducts. In general, it can lead to damage to all facilities in an area affected by the earthquake [5].

Satellite technology can be considered an appropriate solution to eliminate the limitations of field operations [6]. Synthetic aperture radar detects displacement at ground level in the late 1980s, introducing differential interferometric synthetic aperture radar [7] technique. The application of D-InSAR in the study of displacement and deformation of the Earth's surface is a relatively new one which is appropriate for applying this method to earth-deformation studies both on regional and local scales [8-11]. In the field of identification and estimation of land surface displacement by using radar satellite imagery and interferometry techniques, several studies have been carried out as follows:

Using PALSAR radar interferometry,[12] tried to estimate the earthquake fault model and prepared a surface displacement map derived from the 2010 Yushu earthquake in China. They also investigated the dispersion of landslides. The researchers' findings revealed that the most left-leaning surface slip was 166 cm in the distance of 9.9 km from the west and northwest of Yushu, and the length of surface faults was estimated to be about 73 km. The results also showed that the greatest deformation from the earthquake occurred around the epicenter and the Long Yao Lake. To estimate the level of land-based displacement and its geological hazard in the Murcia region of Mexico [13] used 22 radar images of ENVISAT from 2003 to 2010. Their study showed that the displacement of 7-8 cm in east-west or northwest and southeast occurred parallel with the main fault. [14] Investigated the changes of Earth's crust in the Kanto region of Japan, which was affected by the Tohoku earthquake in 2011, and it was estimated by the C band of Envisat-ASAR images and a GPS station. They used the InSAR technique to estimate the displacement of Earth and compared it with the displacement of the GPS station in which RMS was equal to 6.9 mm. The results of these investigations proved the proper use of InSAR for estimating displacement from the earthquake. [15] Investigated chronological and long-term changes of the Arctic regions during 2013-2015. In this regard, Radarsat-2 satellite images and the D-InSAR technique were used. The results showed that the seasonal displacement pattern derived from the D-InSAR technique was compatible with the field observation pattern, and the displacement level was estimated as 1 cm. The researchers' findings showed that the D-InSAR technique was a useful tool for understanding environmental changes in remote areas with hard-to-reach accessibility. [16] Determined the displacement of earthquakes caused by interferometry of ENVISAT satellite images on Qeshm Island. Their study showed that the Earth's displacement along the satellite's view was about 35 centimeters due to the earthquake of 2005 in Qeshm Island. To investigate the displacement of foreshock in Ahar and Varzagan fault by using time series of radar interferometry [17] used StaMPS static dispersion method and 20 radar images from the study area during 2001-2003. The results showed that the maximum level of displacement in the study area was about 9 mm per year [18] determined the amount of displacement caused by the Bam earthquake through ENVISAT radar images. The radar interferometry results in this region showed a 29-centimeter displacement in the west (x), 70 centimeters in the south (y), and 25 centimeters in high levels (z). The accuracy of components in the east, north, and high levels for the 3D displacement field derived from interferometry and azimuth offset technique was 0.9, 9.8, and 8.0 cm, respectively. [19] Studied the subsidence of Rafsanjan plain using D-InSAR and Sentinel-1 satellite imagery. The results of analysis from this time series showed that the region was continuously in subsidence. So, the highest annual subsidence rate with 28 centimeters per year is related to the agricultural land around the district of Bahreman. [20]

The literature review summary refers to the point that remote radar measurement images and the D-InSAR technique are very suitable and applicable for estimating displacement, especially displacement resulting from an earthquake. Therefore, this study aims to identify and determine the trend and rate of land surface changes of the crust in Sarpol-e Zahab city due to the recent earthquake in Kermanshah with the help of Sentinel-1 a remote measurement data.

1.1. The study area

With a surface area of 903.39 km, Sarpol-e Zahab city is located in the range of 46°2' to 45°47' of east longitude and 34°41' to 34°12' of northern latitudes and in the west of Iran and furthermost of Zagros slopes (Fig. 1).

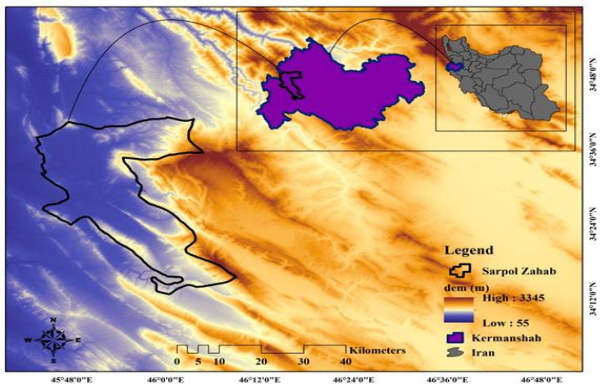

Fig. 1. The study area.

2. Methodology

In the present study, to achieve land changes resulting from an earthquake in Sarpol-e Zahab city, the D-InSAR and SAR images of the Sentinel1-A satellite of European Space Agency [21] by SLC and vv polarization format were used (Table 1). The images used in the Sentinel1-A sensor (with a wavelength of 5.5cm in C band), in terms of spatial resolution, are placed in the range of the sensor with middle spatial resolution. After taking pictures of the study area, the images were processed using the SARscape5.1 plugin in ENVI 5.3 software.

Table 1. The type of images used and prepared by radar Sentinel-1 A.

Shooting history	Orbit	Format	Spatial resolution	Imaging band
2017/10/25	174	IW (Interferometric Wide swath)	5 m x 20 m	C-SAR
2017/11/18	174	IW (Interferometric Wide swath)	5 m x 20 m	C-SAR

Fig. 2 shows the overall trend of the study.

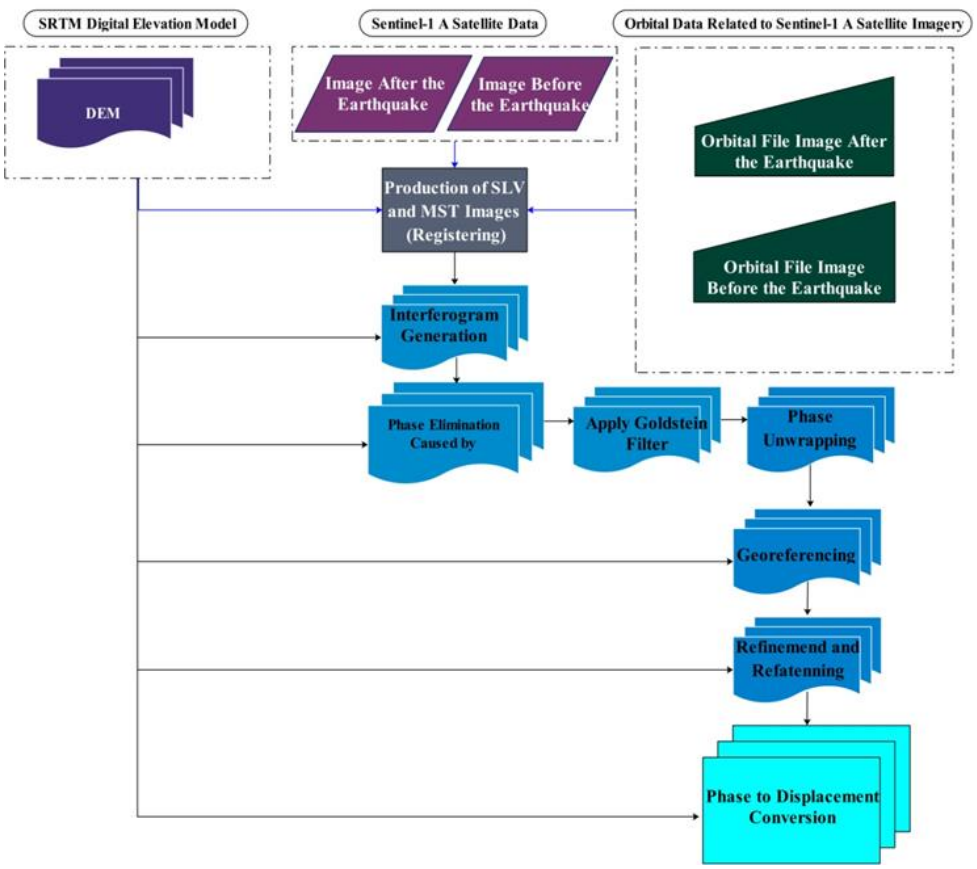

Fig. 2. The overall trend of the study.

The process of unifying the coordinate system of the two SLC images is called image registration. As mentioned, radar coordinates of the platform or platforms should be identified to register images 1 and 2. Unfair alignment in the SAR image reduces the correlation between the two interferometric signals because the correlation function does not take place on the corresponding pixel in the image. Therefore, two images must be registered accurately below the pixel to obtain a high-quality fringe pattern. When two SLC images are registered, the combined multiplication

process is performed to produce interferometer and coherent images.,The radar file of images was prepared, and these two images were registered before and after the earthquake to register the two images compared to each other.

The interferogram contains the phase difference between the two images. Each point in the region is determined at the time of the preparation of two images by examining the phase difference. The interferogram is created by multiplying the original image in a conjugate of the dependent image Eq. (1).

$$I = MS^{*}$$
$$\phi_I = \phi_M - \phi_S \quad (1)$$

Where M refers to the mixed main image (Mater), S refers to the second mixed image (slave), I stands for interferoram, $*$ is mixed conjugate, ϕ_M is image phase (Master), ϕ_S refers to image phase (slave), and ϕ_I stands for interferogram phase.

An interferogram consists of fringe cycles. Two points in a colored strip (with the condition that the path between two colors does not pass any other color) are equally displaced [22]. If the respective area has a height change of zero, the phase difference is constant in the azimuth direction and increases linearly in the board's direction. Moreover, when this difference reaches the value of 2π , it returns to zero, and this process repeats. Hence, the interference pattern of such a region includes horizontal fringes in the direction of the azimuth. This phenomenon is due to a baseline in the board's direction, and its effect should be eliminated, which is known as flat earth correction (To remove the effect of topography, DEM SRTM with a precision of 30 meters is used).

The resulting differential interferometer contains some noise. The factors causing this noise can be different; the two main factors affect their occurrence. The first factor is the time difference between the two main and dependent images. Occasionally, some of the changes in the region that occur between the time intervals of the two images are among the factors that create noise. The second factor is the spatial baseline. The number of noise in the images directly relates to the spatial baseline; the higher the number, the more noise we will encounter in the interferometer. The filter was used to remove these noises. If the filter window is very small, the magnitude of the correlation of pixel will change considerably from one pixel to another; however, if the window is much larger, it will produce a complete result. The coherence image implies the degree of matching between the return signals of the equivalent pixels in the SLC image and is composed of values between zero and one, with larger images (close to 1) indicating closer alignment and more reliability. The complexity created in the raw interferogram is because the differences between the phases shown are not entirely complete in terms of the total number of wavelength cycles but only are measured in terms of a range from 0 to 360 degrees. Each complete cycle shows 0-360 degrees or 0- 2π radians of an interferometric fringe. Absolute phase differences must be corrected or unwrapped by adding appropriate factors before the height is extracted, called phase unwrapping or correction. The problem here is that the difference in work between the received signals is measured by two antennas in the range of radian. An appropriate factor must is added to the calculated phase difference to calculate the actual phase difference. The unwrapped image may contain holes that represent pixels where the coherence of the phase is less than the amount that can be used to calculate phase difference or it may indicate areas of the radar shadow. Therefore, softening or removal of noise can be implemented using a comparative median filter [23] or by using a wavelet transform [24] before the phase unwrapping operation. On this basis, before applying phase unwrapping, the Goldstein filter was executed on an image of the respective area. This filter handles all phases and creates better fringes. Before the final stage, which is the conversion of phase values to height, to improve results of the stage implementation processing, refinement and referencing are necessary. At this stage, all completed actions have been reviewed so far, so that we can obtain an ideal image with the slightest influence of topography and phases and refined satellite circuits. The implementation of this step causes the probable errors of radars to be corrected and the phase offset is calculated, and thus the absolute phase values are obtained.

The final stage, which is the conversion of the absolute phase to the displacement, is called the most important part since the output of this stage represents the degree of land displacement, so the maximum accuracy is applied. The phase change values express that height changes are equal to half of the wavelength, given that the ASAR imaging wavelength is 5.6cm. Changes about 2π are equal to height changes about 2.8 cm. For each pixel, change of phase to height is equal to height change in that point calculated in terms of metric unit, and thus the amount of displacement occurring in the study area is obtained. According to the points mentioned above, regarding the stages of differential radar interferometry and the discussed relationships, the displacement map was generated using Sentinel-1 a sensor images and generated via the SARscape 5.1 plugin in the Envi 5.3 software.

3. Results and Conclusion

Kermanshah earthquake occurred at 9.48 pm on Sunday, November 2017, 35 kilometers away from Sarpol-

e Zahab city, with a magnitude of 7.3, causing financial losses, which can be considered the most disastrous event of the current decade. National Seismological Center affiliated to the Geophysics Institute of Tehran University, International Institute of Earthquake and Earthquake Engineering of Iran, German Earth Sciences Center, Seismological Center in Europe and Mediterranean, and Seismological Center of USA, in their complementary reports, declared that the epicenter of Kermanshah earthquake was in a distance of 10 kilometers in the south of Ozgale and within the borders of Iran at a depth between 18 and 25 kilometers (Table 2).

Table 2. Specifications of the earthquake center with a magnitude of 7.3 in Ozgale, Sarpol-e Zahab in Kermanshah, reported by IRSC and other centers.

Reference	Latitude	Longitude	Depth(km)	Magnitude Richter
IRSC	34/77	45/76	18/1	**7/3**
IIEES	34/88	45/84	18	**7/3**
EMSC	34/79	45/85	24	**7/3**
USGS	34/91	45/96	19	**7/3**
GFZ	34/850	45/9	25	**7/3**

To investigate the changes of the land surface resulting from this event, remote sensing data from Sentinel-1 a radar satellite on November 2, 2017, and November 27, 2017, were used as data sources before and after the earthquake. The analysis of data based on the radar differential interference technique was performed using the SARscape 5.1 plugin. After creating mst and slv images, they were identified with the help of Google Earth Browser software, and four bursts of the respective area were identified (IW1-6, IW1-7, IW1-8, IW1-9), and each of them was processed separately. Fig. 3 shows the interferograms and fringes created in the study area due to an earthquake near Ozgale.

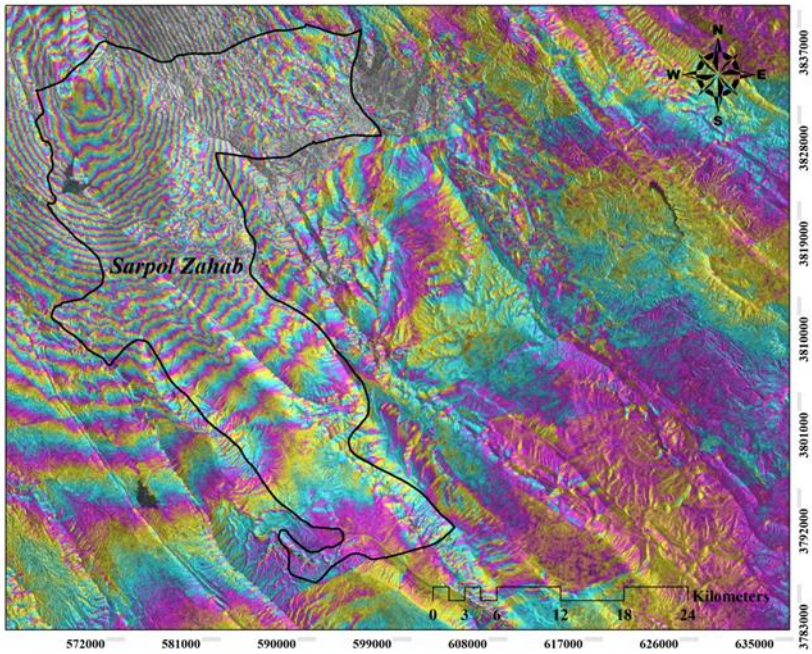

Fig 3. Interferogram and obtained fringe for Sarpol-e Zahab.

As shown in Fig. 3, the fringes formed from the north to the south have an opening trend. The amount of displacement in the north and northwest of Sarpol-e Zahab is more than south and southeast. This map shows that the displacement pattern in Sarpol-e Zahab is from the northwest to the southeast, or in other words, from the epicenter of the earthquake towards Sarpol-e Zahab. This displacement pattern corresponds to the high level of damage observed in Sarpol-e Zahab.

After reviewing and analyzing the interferograms obtained from Sarpol-e Zahab, re-modification and refinement were performed to improve the phases obtained from the study area. Finally, the constructed phases were converted to vertical displacements (Fig. 4).

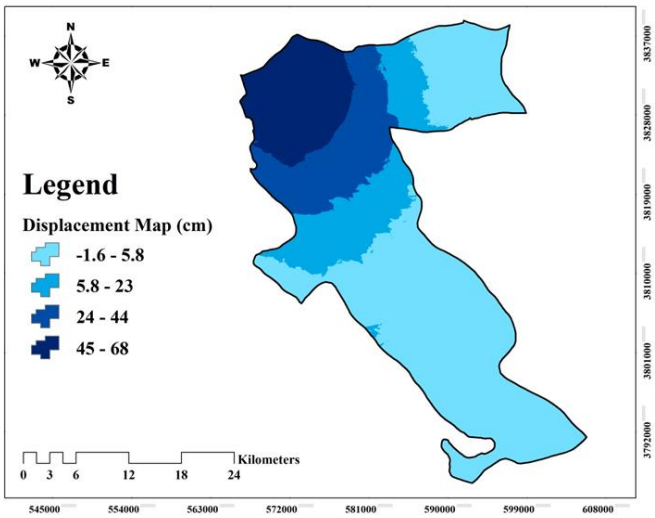

Fig. 4. The displacement rate obtained by Sentinel-1 a data for Sarpol-e Zahab.

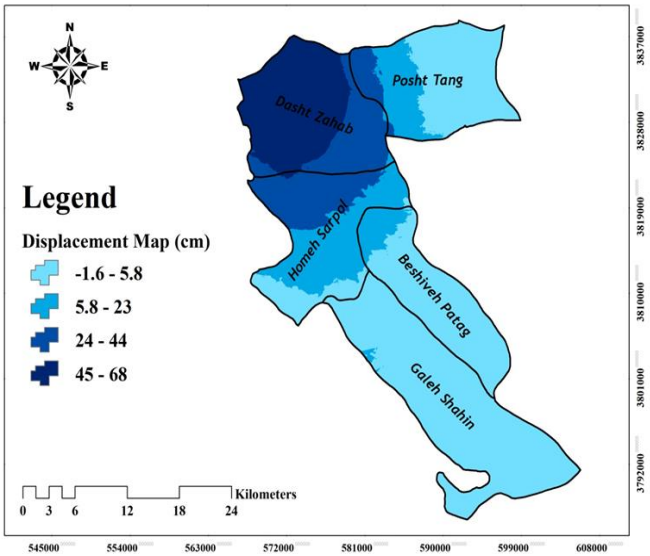

Fig. 5. The relationship between Sarpol-e Zahab villages and the displacement map.

As shown in Fig. 4, the displacement rate in Sarpol-e Zahab is between -1.6 and 68 centimeters. The final displacement map indicates that the north and northwest of the city, with a height of 24-68 cm, had the highest displacement. From total area of Sarpol-e Zahab, the displacement level was 131.20 km (14.52%), between 45-65 cm, 133.19 km2 (14.74%), between 24-44 cm, 145.83 km2 (16.14%), between 5.8-23 cm and 493.14 km2 (54.58%), between -1.6-5.7 cm. It can be said that the north and southwest of Sarpol-e Zahab have had more displacement due to its proximity to the earthquake center.

According to Fig. 5, the villages of Zahab plain, Sarpol suburb, and Posht Tang have the highest displacement, and Beshive Patagh and Shahin Castle have the least displacement. According to the displacement map, Sarpol-e Zahab is prone to a displacement of 5.8-23 cm. examining the relationship between the city and displacement map shows that Sarpol-e Zahab has risen from 5 to 14 cm.

REFERENCES

[1] Sharifi KIA, M. (2010). Analysis of earth crust changes resulting from the earthquake by remote sensing techniques.The 4th International Congress of Geographers of the Islamic World, Zahedan, Sistan and Baluchestan University.

[2] Clanton, U.S., and & Amsbury, D.L., (1975). Active faults in southeastern Harris county. Texas Environmental Geology, 1, 149–154.

[3] Chen, Yang, Shengwen Yu, Qiuxiang Tao, Guolin Liu, Luyao Wang, and Fengyun Wang. "Accuracy Verification and Correction of D-InSAR and SBAS-InSAR in Monitoring Mining Surface Subsidence." Remote Sensing 13, no. 21 (2021): 4365.

[4] Barends, F. B. J., Frits, J. J., Brouwer, H ., & Frans, S ., (1995). Proceedings of the 5th International Symposium On Land Subsidence, The Hague, The Netherlands, No. 234, 16-20.

[5] Heshmi, Sh. (2014). Modeling of subsidence of Neyshabour plain using time series and D-InSAR technique. Unpublished Master's thesis, Islamic Azad University, Yazd, Department of Measurement and Geographic Information Systems.

[6] Shokouhi Nejad, (2016). Determination of earthquake displacement area using radar images (Bam earthquake), Unpublished Master's thesis, Islamic Azad University, Shahrood Branch, Civil Engineering Faculty.

[7] Liu, Xiaobing, and Jilei Huang. "An improved multi-platform stacked D-InSARmethod for monitoring the three-dimensional deformation of the mining area." IEEE Access 9 (2021): 66878-66890.

[8] Hanssen, R.F. (2001). Radar interferometry: Data interpretation and error analysis. In Remote Sensing and Digital Image Processing; Kluwer Academic: Dordrecht, Netherlands, Volume 2.

[9] Hooper, A., Spaans, K., Bekaert, D., Caro Cuenca, M., ArGkan. M., & Oyen, A., (2010). StaMPS/MTI manual; delft institute of earth observation and space systems, Delft University of Technology, 35pp.

[10] Osmanoglu, B. (2011). Application and development of a new algorithm for displacement

analysis using InSAR time series. Unpublished Ph.D. Dissertation, University of Miami.

[11] Roustayi, Sh., Ahmadzadeh, H., Nikjou, M., & Dehghani, M. (2014). Assessment of the location of habitats affected by natural hazards using the differential interferometry technique: A case study of the Googerd village. Journal of Geography and Planning, 20(55), 145-160.

[12] Tobita, M., Nishimura, T., Kobayashi, T., Xiansheng Hao, K., & Shindo, Y., (2011). Estimation of coseismic deformation and a fault model of the 2010 Yushu earthquake using PALSAR interferometry data. Earth and Planetary Science Letters, 307 (3-4), 430–438.

[13] Cigna, F., Osmanoğlu, B., Cabral-Cano, E., Dixon, T., Olivera- Ávila, J. A., Garduño-Monroy, V. H., DeMets, Ch., & Wdowinski, Sh., (2012). Monitoring land subsidence and its induced geological hazard with Synthetic Aperture Radar Interferometry: A case study in Morelia, Mexico. Remote Sensing of Environment, 117, 146–161.

[14] Eigharbawi, T., & Tamura, M., (2015). Coseismic and postseismic deformation estimation of the 2011 Tohoku earthquake in Kanto Region, Japan using InSAR time series analysis and GPS. Remote Sensing of Environment, 168, 374-387.

[15] Rudy, A. C. A., Lamoureux, S. F., Treits, P., Short, N., & Brisco, B (2018). Seasonal and multi-year surface displacements measured by D-INSAR in a high Arctic permafrost environment. International Journal of Applied Earth Observation and Geoinformation, 64, 51-61.

[16] Akbari Mehr, M., & Rajabi, B. (2011). Determination of displacement field resulting from an earthquake by using radar satellite interferometry. The 6th International Conference on Earthquake Engineering and Seismology, Tehran, International Institute of Seismology and Earthquake Engineering.

[17] Saadatfar, A., Dehghani, M., Esmaeili, A. & Zamani Qara Chamani, B. (2014). Investigation of displacement in foreshock of Ahar-Varzaghan fault using radar interferometry time series. Journal of Radar, 2(2), 11-20.

[18] Shokouhi Nejad, (2016). Determination of earthquake displacement area using radar images (Bam earthquake), Unpublished Master's thesis, Islamic Azad University, Shahrood Branch, Civil Engineering Faculty.

[19] Roozban, A. (2016). Investigate earth subsidence using differential radar interferometry (D-INSAR) technique by using Sentinel's New Sensor Image. Unpublished Master's thesis, Industrial and Advanced Technological University, Faculty of Civil Engineering and Mapping.

[20] Meng, Xing-min, Tian-jun Qi, Yan Zhao, Tom Dijkstra, Wei Shi, Yin-fei Luo, Yuan-zhao Wu et al. "Deformation of the Zhangjiazhuang high-speed railway tunnel: An analysis of causal mechanisms using geomorphological surveys and D-InSAR monitoring." Journal of Mountain Science 18, no. 7 (2021): 1920-1936.

[21] European Space Agency (ESA), Missions: Sentinel, 2016, http://sentinel.esa.int/web/sentinel/missions/sentinel-1.

[22] Rahnmoun, M., Serajean, M., & Rahmati, M., (2005). Using radar interferometry in Bam earthquake and IZMIT earthquake study in Turkey. Geomatics conference 84, Mapping Organization.

[23] Premelatha, M. (2001). Quality assessment of interferometrically derived digital elevation models. Unpublished Ph.D. Dissertation, University of Nottingham.

[24] Braunich, H., Wu, B., & Kong, J. A. (2000). Phase unwrapping of SAR interferograms after wavelet denoising. Proceedings of IEEE International Geoscience and Remote Sensing Symposium (IGRASS), Honolulu, Hawaii, New York: IEEE, 752-754.